Improved Design of a Gait Rehabilitation Robot

C. J. Stolle[1], C. A. Nelson[1], J. M. Burnfield[2], and T. W. Buster[2]

[1]*University of Nebraska-Lincoln, USA, e-mail:cale.stolle@huskers.unl.edu; cnelson5@unl.edu*

[2]*Madonna Rehabilitation Hospital, USA, e-mail: jburnfield@madonna.org; tbuster@madonna.org*

Abstract. Gait therapy is important to a person's recovery following spinal cord or brain injury, stroke, lower extremity surgery, as well as with many chronic conditions (e.g., Parkinson's disease or multiple sclerosis). Although some affordable equipment for adult gait rehabilitation exists, such equipment for adaptive gait rehabilitation across the spectrum of pediatric sizes is not commercially available. This paper presents design improvements for a new pediatric gait rehabilitation machine intended to address this technology gap. The design is in the style of elliptical machines but is synthesized to emulate the normal kinematic demands of walking. It includes a 7-bar linkage for each foot, a chain/sprocket coupling for left/right synchronization, and motorized speed control.

Keywords: Gait rehabilitation, pediatric gait, robotic rehabilitation, kinematic synthesis.

1 Introduction

Gait rehabilitation typically constitutes part of the therapy needed following spinal cord injury, brain injury, or other conditions affecting motor coordination. For adults, various forms of therapy are available, including treadmill training with partial body-weight support [1], robotic guidance of the legs [2], and assistive elliptical machines [3-6]. These therapeutic approaches all have different advantages, but with limited exceptions [3] they are very costly either based on the equipment or personnel needed. Furthermore, affordable therapies for pediatric patients [7] are very limited, in part because the equipment is designed for specific ranges of motion (or step length), and pediatric patients can have step lengths which vary more than can be accommodated by typical equipment. Therefore, there is a need for gait therapy devices which are adaptable to the full spectrum of step lengths while remaining affordable for widespread clinical adoption.

A pediatric gait training device was recently proposed [8] to fill this need. A device was constructed comprising carriages riding on two pivoting rails, as shown in Figure 1. The carriages propelled the foot through a gait-like motion. To model the motion of the toe, the carriages slid along the rail as the rail pivoted on

a central axle. To model the motion of the heel, which in turn drives the angle and motion of the rest of the foot, the back of the carriage rolled along another rail that translated vertically. The forward and backward sliding of the carriages was controlled by a pair of identical four-bar linkages. The pivoting of the rails was controlled by cams, and the timing of all these elements of motion was synchronized using timing belts. A line diagram of power transmission in the robot design is shown in Figure 2.

Fig 1 Initial Prototype of Gait Rehabilitation Robot (as in [8])

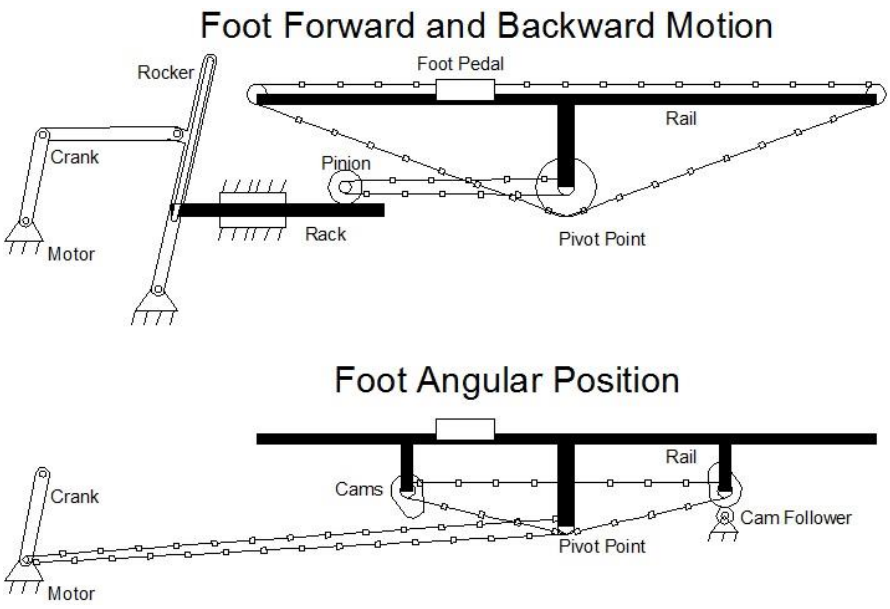

Fig 2 Power Transmission in Gait Rehabilitation Robot (as in [8])

The initial design proved overly complex for practical implementation and suffered from excessive frictional losses due to the large number of mechanical interconnections. In this paper we present a new design for scale-adaptable robotic gait rehabilitation. The original design is assessed and critically evaluated in terms of the original design goals. Emphases were made on assessing any modifications and their impact on scaling and overall foot trajectory. From this assessment, a new design was proposed and implemented.

2 Design Requirements

The initial design needed to be simplified in order to be functional. The primary design goals were assessed.

- The robot must propel the foot through a gait-like trajectory. The trajectory does not have to be exact, but significantly closer to walking mechanics compared with other low-cost gait-simulating machines.
- The robot must have scalable output so that pediatric and adult patients are able to use it.

Secondary design goals were also reviewed:

- Small footprint
- Comfortable for the patient
- Smooth and easy to operate
- Cost efficient

While most of these goals were achieved in the original design, the greatest deficiency of the design was in smoothness and ease of operation. It was determined that in order to achieve improved performance in this regard, and simultaneously reduce cost and complexity, some modest decreases in satisfaction of the other requirements may be acceptable.

3 Initial Design

An initial design was constructed according to the design goals listed above, and is detailed in [8]. We summarize here some of its design features for comparison.

3.1 Motion Scaling

The design needed to accommodate various stride lengths of users. Ideally, the scaling would be perfectly linear. This would provide consistency of foot path shape as the stride length is changed from short to large. The scaling mechanism

must be fairly robust and reliable at each scaling value in order to function properly.

There are multiple ways of achieving scalable motion using mechanisms. By using a four-bar linkage with variable link lengths, the output could be manipulated to produce the same trajectory shape. However, since all four links would have to be simultaneously adjusted to maintain proportions, this was not pursued as a scaling mechanism. Similar issues were present if using a pantograph. Attempts at Cartesian parametrization also proved difficult. These options are explained in more detail in [8].

One approach is to parametrize the motion path in polar coordinates. This expresses the path as a function of angular displacement, with radius as the primary variable. When scaling such a curve, the angular position remains the same while the radial distance scales. This allows the scaling problem to be limited to one independent variable. The polar parametrization can be realized through a slider on a pivoting rail where the pivot serves as the fixed point about which trajectories are scaled.

The initial design utilized a carriage travelling on top of the rail, where the rail was pivoted about a central axis. The forward and backward motion of the carriage was controlled by the rocker of a four-bar linkage. The rocker contained a slot to allow for a wheel to travel inside of it. The lateral deflection of the wheel was lengthened by increasing the distance between the pivot point and the wheel's axle. Since the relationship between radius and distance are linear at fixed angular deflections, this would provide an even, smooth scaling for the system.

The follower wheel was attached to a gear rack which was constrained to only move horizontally, as shown in Figure 3. The rack meshed with a pinion to convert the horizontal oscillatory motion to a rotary motion. The rotary motion was transmitted to a belt to drive the foot carriage, which converted it back to a linear motion. This chain of conversions allowed the carriages to be positioned anywhere relative to the follower wheel on the rocker.

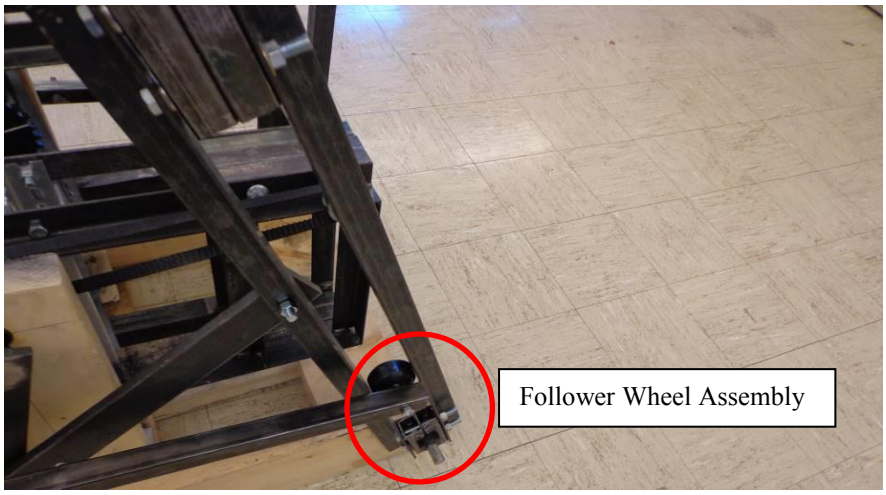

Fig 3 Rocker and Follower Wheel

3.3 Gait-Like Motion

The main purpose of this design effort was to develop a robot that replicated the motion of the foot during a normal gait cycle. The expectation was that this would help to drive a normal gait pattern in rehabilitation patients using the machine. This could be realized by fully constraining the foot motion to match the foot trajectory of a sample gait path at both the metatarsal and heel positions, as shown in Figure 4. Both the metatarsal and heel trajectories were measured relative to the forward motion of the individual as determined by the position of the hip. The trajectories were measured using motion-tracking software and an infrared camera system.

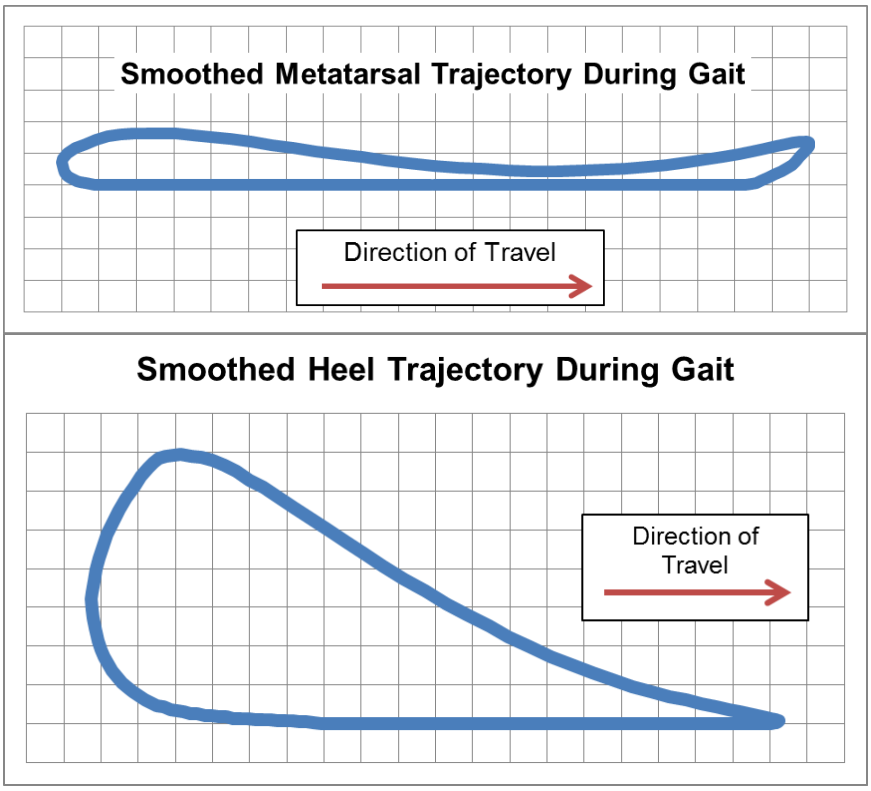

Fig 4 Sample Metatarsal and Heel Trajectories During Gait

As stated in Section 3.1, it was determined that the foot trajectory would be traced with a crank-slider mechanism. However, neither the metatarsal nor heel trajectories would be feasible to model with a crank-slider system using a polar coordinate system because conversion of the trajectories shown in Figure 4 resulted in angular accelerations that were excessive for an actual mechanism. A sample of the radial and angular accelerations for the metatarsal trajectory, with the pivot point of the rail located in front of the furthest forward point of the toe, is shown in Figure 5.

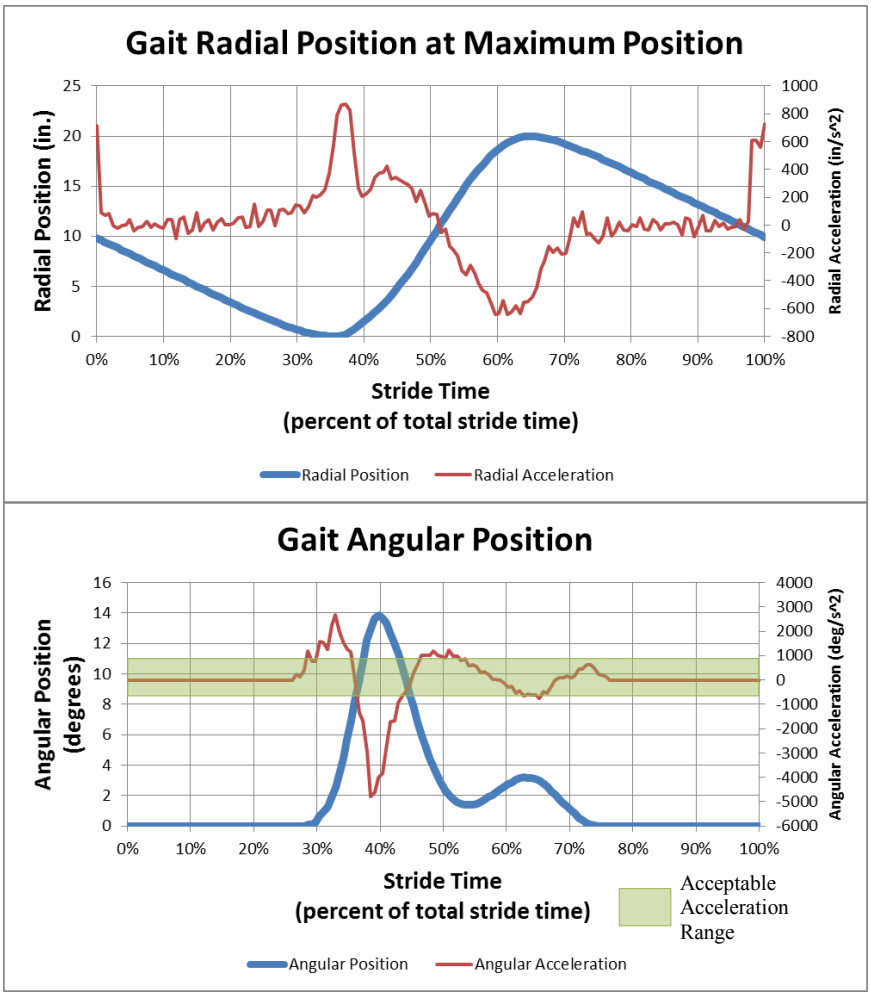

Fig 5 Radial and Angular Position and Acceleration of Gait Cycle

To model human gait patterns, a projected point on the foot had to travel through a trajectory that could be modeled in polar coordinates and realized as a crank-slider system. This was determined by interpolating the trajectory of a point on the foot using the X and Y position of the metatarsal and heel points. A 2-dimensional profile was generated as a function of the position of the foot based on the heel and metatarsal trajectories. This assumed the connection between the heel and metatarsal was rigid. Based on this analysis, it was determined that a point on the foot located slightly in front of the toe has a self-intersecting trajectory with tangency near the middle of the trajectory, as shown in Figure 6. This intersection minimizes the rail motion while providing biomechanically accurate motion of one point on the foot.

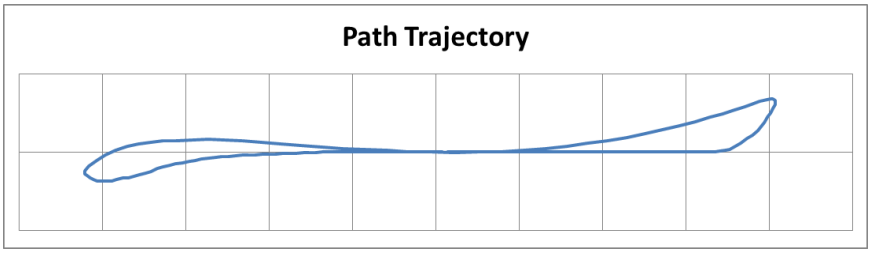

Fig 6 Crank-Slider Compatible Path Trajectory

3.4 Path Generation

For the initial design [8], the trajectory was recreated using a pivoted rail. Since the crank-slider trajectory experienced relatively small angular deflection (reaching a maximum value of 9.6 degrees and a minimum value of -3.5 degrees relative to horizontal), cams were chosen to drive the pivoting motion of the rail. A four-bar linkage was used to drive the forward and backward motion of the slider carriage.

The maximum speed of the machine was chosen to be approximately one stride (one left and one right step) per second. Treating the rail as a cam-follower, acceleration analysis indicated that the rail would "hop" due to downward accelerations exceeding the gravitation constant. To reduce vibrations in the system, the cam profile was manually adjusted to limit accelerations to 330 in/s^2. The velocity and displacement of the end of the path was adjusted accordingly with the new acceleration profile.

The rail and carriage configuration and the angular position described in Figure 6 only constrained a point on the foot in front of the toe. In order to fully constrain the foot, a design feature was created that incorporated a secondary motion-constrained point on the foot pedal. It was decided that secondary cams would drive the vertical motion of a bar extended across the length of the pivoting rail. A wheel connected to the rear of the foot carriage would follow the bar and constrain the rise and fall of the heel. Similar to the toe cam profile, the heel cam profile was acceleration-limited to 330 in/s^2.

4 Shortcomings of Initial Design

As mentioned previously, the initial design did not function properly. The mechanism did not move under human power as intended.

4.1 Deficiencies in the Initial Motion Scaling Design

After construction, the system proved impractical due to the excessive force required to drive it. The frictional losses at the rack and pinion and at other mechanical interconnections were significant, making the conversion between linear and rotary motion inefficient. Attempting to directly connect the follower wheel to the carriage required significantly more constraint on the follower wheel, and this jammed the system. This occurred because the follower wheel was poorly constrained and the connection with the rocker of the four-bar linkage was not sufficiently precise.

While methods could have been employed to significantly strengthen the constraints on the follower wheel, it would not have decreased the power losses at the pinion. Furthermore, tooth contact in the spur-type pinion-rack mesh was noisy and was anticipated to create a poor user experience.

4.2 Limitations of Initial Path Generation Design

While the accelerations of the cam were slightly below the gravitational constant, the cams produced large forces on the rail. Furthermore, the somewhat severe profile of the cam meant that the cam follower experienced questionable pressure angles, causing the device to be difficult to drive without significant torque.

The axle driving the heel was also integrally linked to the rest of the system. The high accelerations experienced by the heel required high torque to overcome the steep cam slopes. The combination of these two sets of cams was ultimately too much for the system to drive, and caused the system to seize.

5 Description of Revised Design

Following the failure of the first design, the goals of the design were reevaluated and used to create a new robot. The new robot had to have significantly improved power transmission over the initial design, and the motion scaling and path generation would need to be changed.

The new design consisted of a seven-bar linkage with an additional cam constraint. A crank-rocker four-bar linkage formed the foundation of the design. A block slid along the rocker, and could be fixed in place with a pin. The block was attached to a bar that connected to a carriage. The block and bar assembly is shown in Figure 7. This carriage carried the off-axis loading from the linkage and transmitted it into longitudinal motion along a pivoting rail. With cams driving the angular displacement of the pivoting rails, and the cam rotation coupled to the crank of the four-bar, this forms a cam-constrained seven-bar linkage with one

DOF. The schematic of the robot and the line diagram for power transmission is shown in Figure 8. A picture of the assembled robot is shown in Figure 9.

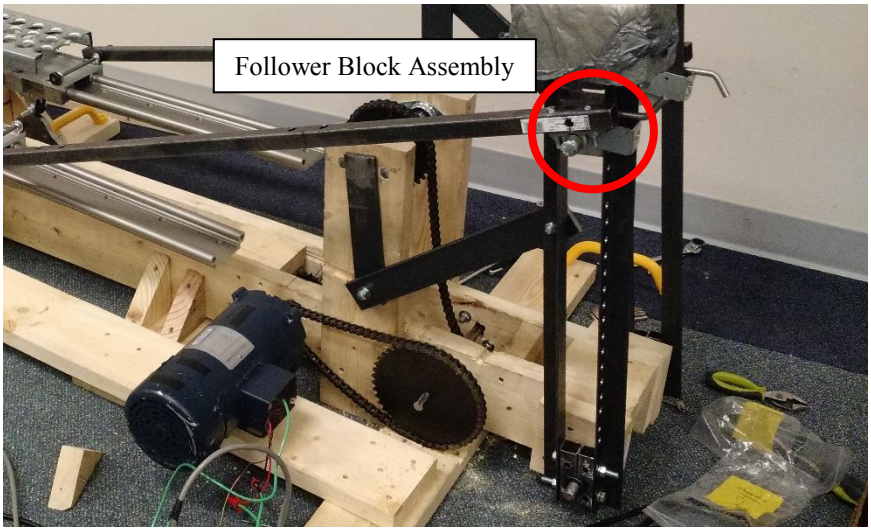

Fig 7 Follower Block Assembly on Crank-Rocker

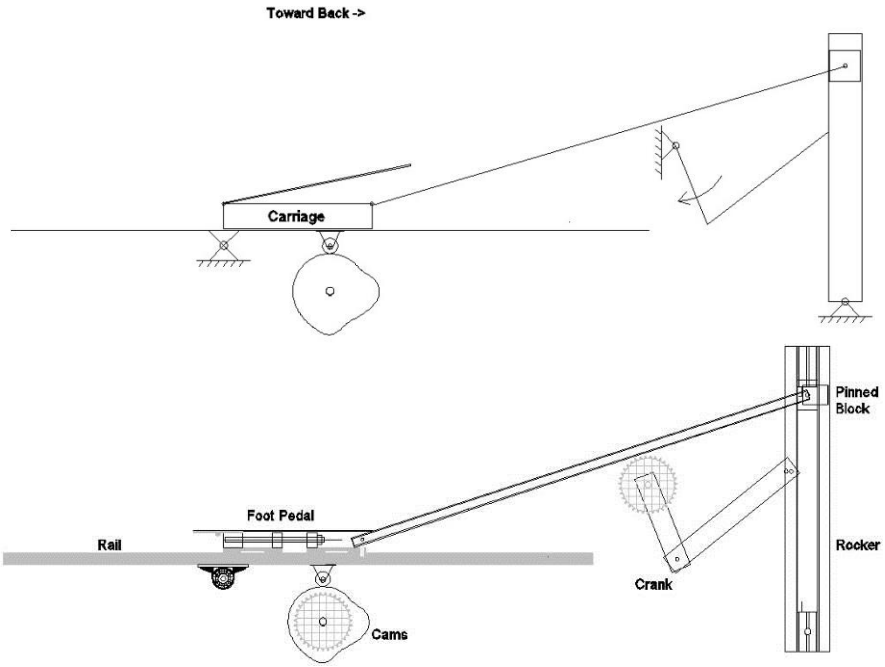

Fig 8 Revised Design Schematic Diagram and Component Models

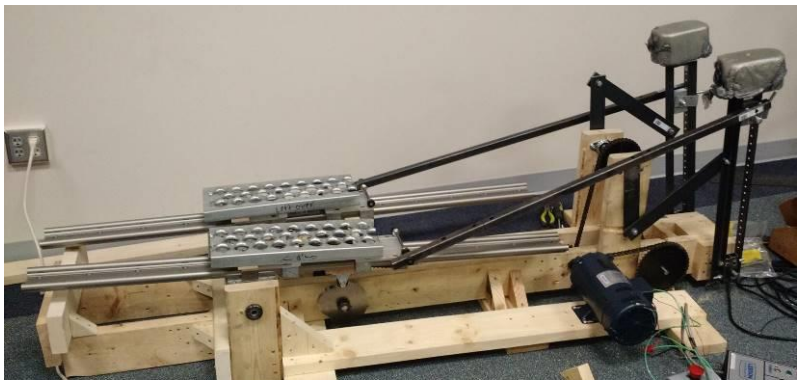

Fig 9 Prototype Based on Revised Design

5.1 Improved Motion Scaling Design

Unfortunately, as per the first design, it would not be possible to have a well-constrained follower wheel and connection linkage to the carriage while maintaining perfect scaling at every length along the rocker. Thus, a significantly simplified connection between the rocker and the carriage was designed. A block was pinned into position on the rocker arm, as shown in Figure 7. A linkage connected the pinned block rigidly to the carriage. One drawback of this design was that changing the position of the pinned block in the rocker changed the distance between the block and the centerline of the rail, meaning that the carriage would trace an inaccurate trajectory. To compensate for this, the connection between the pinned block and the carriage was adjustable. After setting the block at the desired height along the rocker (which would, in turn, regulate the stride length of the robot), the link between carriages was adjusted so that the foot pedal was aligned correctly with the pivot point to achieve the correct trajectory.

5.2 Improved Path Generation Design

During the terminal stance and pre-swing phases of a normal gait cycle, the heel naturally rises, enabling the body to pivot over the forefoot [9]. Then, during initial swing, the toes and forefoot begin to elevate to ensure foot clearance. By mid-swing, as the tibia achieves a vertical position, the toes and heel align parallel to the ground allowing only a minimal threshold for foot clearance. By terminal swing, the toes are again elevated relative to the heel as the foot prepares for a heel first initial contact. This implies that it is desirable to avoid constraining the heel, as it naturally lifts during the latter half of stance, and the slope of the rail during early swing phase is such that the heel would be slightly elevated. Thus, it

was decided that the prescriptive constraint of heel motion would be removed from the design requirements.

The cam profiles experienced excessive accelerations in the initial design. Thus, the cam profiles were reduced to further limit the accelerations. For the new design, the cams were limited to a peak acceleration of 220 in/s^2. The desired profile, initial design accelerations, and second design accelerations are shown in Figure 10.

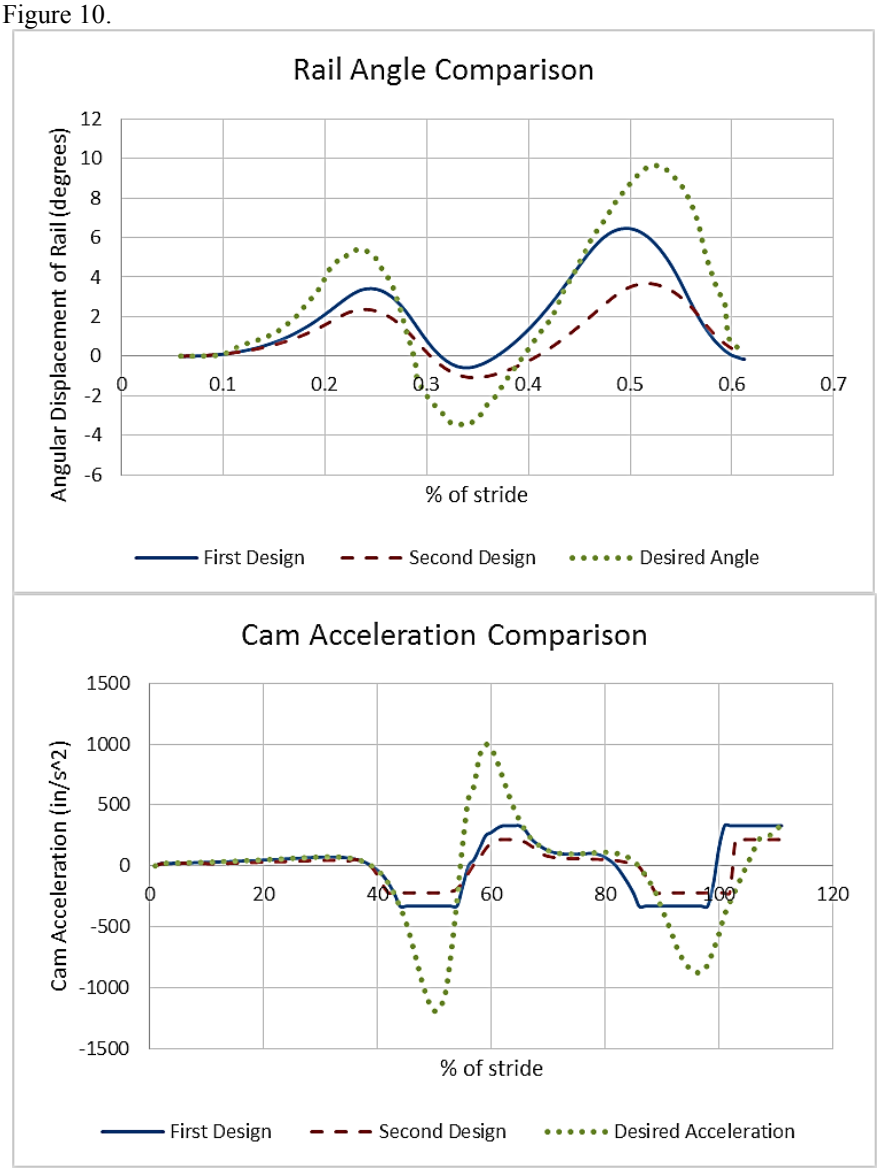

Fig 10 Rail Angular Displacement and Acceleration Comparison

The peak angular displacement values and the times at which they occur in the gait cycle are important to the performance of the robot. Peak times and displacements from the desired toe trajectory, the initial design, and the revised design are compared in Table 1. Overall, based on the data presented in the table, the new design showed slightly reduced fidelity to typical walking biomechanics compared to the first design. However, the increase in system stability and overall performance and usability were significant.

Table 1 Peak Timing (% gait cycle) and Angular Displacements (degrees) of Toe Trajectory

	Peak Description	**1st Positive Peak**	**Negative Peak**	**2nd Positive Peak**
Peak Times (% gait cycle)	Old Profile	24.5	33.9	49.6
	New Profile	24.0	34.7	51.7
	Desired Profile	*24.5*	*32.8*	*52.5*
Peak Angle (degrees)	Old Profile	3.42	-0.57	6.46
	New Profile	2.36	-1.09	3.66
	Desired Profile	5.19	-3.47	9.69

While the first design used large, bulky rails, removing the heel constraint allowed the rails to become significantly thinner and lighter in the revised design. It was decided that standard linear motion bearings would be used for this design, which would significantly reduce the time and effort required to construct the foot-pedal carriages while ensuring quality and weight capacity.

The same four-bar linkage and rocker were used on the new design. It was determined that, due to the oscillatory nature of the foot strides, the machine became stuck at the toggle positions of the crank and coupler. These positions coincided with the maximum and minimum stride positions of the carriages, which are points at which it is difficult (and feels unnatural) to apply forces from the feet to the pedals to drive the system. Thus, a motor was installed to ensure the robot moved smoothly through these toggle positions and generated overall motion consistent with normal human gait; this is also consistent with our goal of using this system for rehabilitation (patients will typically require motorized assistance). Synchronization of the 4-bar linkages and cams is achieved using a chain and sprockets as opposed to the timing belts in the initial design. The design schematic is shown in Figure 8, and the constructed machine is shown in Figure 9.

Conclusions

Based on development of a pediatric gait therapy device, analysis of the design showed that there were several inadequacies. The cam shapes had excessively

large accelerations, which translated to significant torque on the system. The connections to the carriages driving the sliding motion were inefficient. The mechanisms to constrain the heel motion during a gait cycle were excessive. These issues were resolved by simplifying the design and changing the cam profiles, leading to a redesigned gait rehabilitation robot. Preliminary testing of the new prototype system shows greatly improved performance. Future work will include testing the system with human subjects to assess the benefits of the system for gait rehabilitation.

References

1. Dodd, K. J., and Foley, S.: Partial body-weight-supported treadmill training can improve walking in children with cerebral palsy: a clinical controlled trial. Developmental Medicine & Child Neurology, 49(2), 101-105 (2007)
2. Hidler, J., Wisman, W., and Neckel, N.: Kinematic trajectories while walking within the Lokomat robotic gait-orthosis. Clinical Biomechanics, 23(10), 1251-1259 (2008)
3. Nelson, C. A., Burnfield, J. M., Shu, Y., Buster, T. W., Taylor, A. P., and Graham, A.: Modified Elliptical Machine Motor-Drive Design for Assistive Gait Rehabilitation. J. Med. Devices, 5(2), 021001-021001-7 (2011)
4. Burnfield, J. M., Shu, Y., Buster, T. W., Taylor, A., and Nelson, C. A.: Impact of elliptical trainer ergonomic modifications on perceptions of safety, comfort, workout and usability by individuals with physical disabilities and chronic conditions. Physical Therapy, 91(11), 1604-1617 (2011)
5. Burnfield, J. M., Irons, S. L., Buster, T. W., Taylor, A. P., Hildner, G. A., and Shu, Y.: Comparative analysis of speed's impact on muscle demands during partial body weight support motor-assisted elliptical training. Gait and Posture, 39(1), 314-320 (2014)
6. Burnfield, J. M., Shu, Y., Buster, T. W., and Taylor, A. P.: Similarity of joint kinematics and muscle demands between elliptical training and walking: Implications for practice. Physical Therapy, 90(2), 289-305 (2010)
7. Meyer-Heim, A., Borggraefe, I., Ammann-Reiffer, C., Berweck, S., Sennhauser, F. H., Colombo, G., Knecht, B., and Heinen, F.: Feasibility of Robotic-Assisted Locomotor Training in Children with Central Gait Impairment. Developmental Medicine & Child Neurology, 49, 900-906 (2007)
8. Stolle, C. J., Nelson, C. A., Burnfield, J. M., and Buster, T. W.: Synthesis of a Rehabilitation Mechanism Replicating Normal Gait. In: Proc. of the 14th World Congress in Mechanism and Machine Science, Taipei, Taiwan, 25-30 October (2015)
9. Perry, J., Burnfield, J.M. Gait Analysis, Normal and Pathologic Function, 2nd Edition. Slack: Thorofare, NJ (2010)